Author accepted manuscript version of the publication in
IEEE Transactions on Cognitive Communications and Networking, volume 10, issue 2, April 2024.
Published version: https://doi.org/10.1109/TCCN.2023.3335350

Dynamic Spectrum Management and Routing Solutions for Multi-Radio Mobile Ad Hoc Networks

Arne Lie, *Member, IEEE*, Jan Erik Håkegård, Tore Ulversøy, Vincent Le Nir, Ulf Sterner, Anders Hansson, Harri Saarnisaari, *Senior Member, IEEE*, Tuomas Paso, Timo Bräysy, Juho Markkula, Elisabeth Löfsved, and Jarosław Krygier

***Abstract*—The electromagnetic spectrum's scarcity, the tactical edge's dynamic nature, and the variety of tactical operations impose challenges to military cognitive radio networks. Multi-radio dynamic spectrum management (DSM) and routing promise to increase the spectral efficiency and robustness of tactical ad hoc networks by adding key control plane tools that adapt the network to the varying harsh tactical environments. This paper describes a novel concept where implicit spectrum sensing, a distributed DSM architecture with ontology-based spectrum access policies, modified routing and network time synchronization capabilities interplay to address those challenges. The simulation results verify the designed functionality in harsh electromagnetic environments in a multitude of scenario sizes, in terms of number of radio terminals and number of networks. In particular, the simulation of a large operational scenario shows solid scaling capabilities and that ongoing jamming in several networks is efficiently mitigated and low-loss performance are re-established.**

***Index Terms*—Spectrum, sensing, reasoning, routing, synchronization.**

I. Introduction

DYNAMIC spectrum management (DSM) is supposed to provide improvements over today's fixed frequency allocation in highly dynamic and electromagnetically harsh environments. The DSM potential include increased capacity and connectivity robustness, even in scenarios where the available electromagnetic spectrum is limited, or exhibit challenging conditions due to frequency planning of military coalition operations. Cognitive radio networks are envisioned to provide high bandwidth to mobile users via heterogeneous wireless architectures through DSM [1], [2]. Due to the dynamic nature of the tactical edge and the diversity of tactical operations, the mobile ad hoc network (MANET) technology is considered fundamental for such networks [3], [4].

Tactical edge networks are composed of a variety of platforms (e.g., soldier, UAV, vehicular) and software-defined multi-band radios (e.g., HF, VHF, UHF, SATCOM). Although information can be relayed between these heterogeneous networks through gateways, the capacity of multi-radio terminals is not fully exploited before DSM and routing entities include the multi-radio interfaces into their algorithms. By also adding the concept of time synchronization across networks, these entities will enable a new level of spectrum efficiency, since frequency orthogonality can be obtained between neighbor networks applying frequency hopping in overlapping bands.

This paper presents a radio architecture incorporating integrated wideband sensing, DSM and routing cooperation, and network time synchronization across networks. It also presents specific solutions and simulator implementation blocks for each of these architectural elements. The wideband sensing entity exploits silent periods in the physical layers of the VHF and UHF frequency hopping waveforms, thus achieving its goals without any delay induced overhead. Sensing detection events signal the start of DSM functionality, which also notifies the routing entity about ongoing mitigation actions. In particular, the paper investigates how the proposed architecture performs in environments being exposed by static jammers. Other types of malicious users, such as smart jammers or users falsifying the sensing results, are not considered, as they were out-of-scope for the supporting project. The paper is also constrained to one type of collaborating waveforms in each band.

The outline of the paper is the following: Related work is presented in Section II. The multi-waveform MANET characteristics and challenges are given in Section III, followed by a detailed description of the selected architecture of DSM, synchronization, and routing in Sections IV–VI, respectively. The validation of functionality and performance of selected

Manuscript received 27 February 2023; revised 10 October 2023; accepted 13 November 2023. Date of publication 28 November 2023; date of current version 9 April 2024. This research has been supported by European Defence Agency (EDA) project "Multi band efficient networks for ad hoc networks" (MAENA, 2018–21, ref. no. B-1476-IAP4-GP). The associate editor coordinating the review of this article and approving it for publication was L. Wang. *(Corresponding author: Arne Lie.)*

Arne Lie and Jan Erik Håkegård are with the Department of Sustainable Communication Technologies, SINTEF Digital, 7465 Trondheim, Norway (e-mail: arne.lie@sintef.no; jan.e.hakegard@sintef.no).

Tore Ulversøy is with the Strategic Analyses and Joint Systems Department, Norwegian Defence Research Establishment, 2027 Kjeller, Norway (e-mail: tore.ulversoy@ffi.no).

Vincent Le Nir is with the Department Communication, Information Systems & Sensors (CISS), Royal Military Academy, 1000 Bruxelles, Belgium (e-mail: vincent.lenir@rma.ac.be).

Ulf Sterner and Anders Hansson are with the Department for Robust Radio Communications, Swedish Defence Research Agency Linköping, 581 11 Linköping, Swedan (e-mail: ulf.sterner@foi.se; anders.hansson@foi.se).

Harri Saarnisaari, Tuomas Paso, Timo Bräysy, and Juho Markkula are with the Centre for Wireless Communications, University of Oulu, 90014 Oulu, Finland (e-mail: harri.saarnisaari@oulu.fi; tuomas.paso@oulu.fi; timo.braysy@oulu.fi; juho.markkula@oulu.fi).

Elisabeth Löfsved is with the Communications Research and Product Development Team, Business Area Digital Battlespace Solutions, Saab AB Linkoping, 581 88 Linköping, Swedan (e-mail: elisabeth.lofsved@saabgroup.se).

Jarosław Krygier is with the Electronics Department, Military University of Technology, 00-908 Warsaw, Poland (e-mail: jaroslaw.krygier@wat.edu.pl).

Digital Object Identifier 10.1109/TCCN.2023.3335350

network architectures are given as simulation results in Section VII, before finalizing the paper with conclusions in Section VIII.

II. Related Work

After Mitola's groundbreaking work [5], there has been extensive research on dynamic use of spectrum, where approaches have ranged from opportunistic access based on sensing the spectrum environment locally all the way to fully coordinated DSM through central decision makers such as spectrum brokers [6]. Going from current spectrum management procedures to DSM is, however, very much still ongoing work [7].

The DSM architecture proposed in our publication was a collaborative part of the EDA MAENA project [8][1] The MAENA simulator enables detailed simulation of VHF and UHF networks all the way down to propagation and signal processing levels using IQ-sample representation [8]. Other papers that provide results from the MAENA program include [9], [10], [11], [12], [13]. The MAENA work builds on the EDA CORASMA [14] project. This paper adds to the contributions from these other MAENA related publications by providing a unique DSM solution for combined VHF and UHF networks and a unique composition of innovative solutions from the authoring partners, for the full VHF+UHF DSM, wideband sensing, routing, and time synchronization functionalities. It further provides detailed simulation results for this integration of solutions, for a comprehensive VHF and UHF communications military scenario that also includes jammers.

Part of the DSM solutions use the Satisfaction Equilibrium [15], which has previously been applied to spectrum selection and resource distribution in wireless communication by several authors, e.g., [16]. In our work, a satisfaction algorithm is adapted to the frequency hopping waveforms in the simulator. The algorithm is also augmented with a unique geographic conflict resolution criterion, and it is evaluated through full-scenario simulations whether this conflict resolution criterion may improve the total throughput.

Another part of the DSM solutions, see Section IV, use ontology and policy-based DSM, using the Web Ontology Language (OWL) [17] and SWRL [18] and the SWRL API [19]. The use of ontologies and knowledge processing in radios was demonstrated already by Mitola [5]. Two DARPA dynamic spectrum projects advanced ontology and policy-based spectrum selection [20], [21]. Examples of publications specifically suggesting OWL+SWRL are [22], [23]. A further list of references to ontology-based DSM may be found in [24]. The recent IEEE 1900.5.1 Policy Language for Dynamic Spectrum Access Systems standard is based on OWL 2, but with a specific W3C standardized Rule Interchange Format (RIF), RIF-SCM [25]. In the work in MAENA, a custom ontology was developed. Also, unlike in [20], [21] where a reasoner directly provides frequency decisions, the reasoning provides candidate frequencies to the local fast satisfaction algorithm, as explained in Section IV.

[1]Besides the partners authoring this paper, the MAENA team also consisted of Thales France (coordinator), Thales Germany, Rohde & Schwarz, and Fraunhofer FKIE.

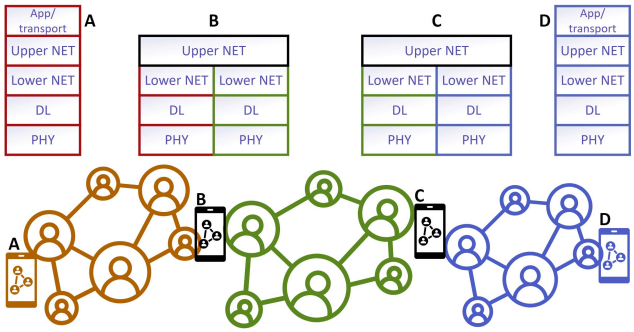

Fig. 1. Radio A can reach radio D via B and C acting as gateways connecting three different MANETs.

Further references to prior work related to the various individual solutions that are employed in the simulations can be found in the description of these solutions in Section IV.

III. Multi-Radio MANET Characteristics

In our study, the MANETs could operate in either VHF or UHF band, and each radio terminal had 1–4 air interfaces in any combination of VHF and UHF. Figure 1 shows three MANETs (colored red, green, and blue) that are using either VHF or UHF waveforms, and the layering approach of the multi-radio network. The Lower NET is a routing protocol and forwarding functionality inside each MANET, and is thus an integral part of the waveform itself. The Upper NET is a routing protocol and forwarding functionality on top of that, dedicated to the internetworking, i.e., establishing forwarding tables that understand how the packets should be forwarded into another MANET. To support user A to user D communication, the Upper NET must provide forwarding tables in all such gateway radios, in this case, radio B and C. The more multi-radio terminals, the more flexible and reliable such interconnections will become. In a dynamic environment, with mobile users and electromagnetic interference, the challenge for the Upper NET is to keep the forwarding tables updated with an adequate compromise between control traffic load and update frequency.

The spectrum resources assigned to each frequency hopping MANET is assumed initially agreed and used as their initial hopsets, but there could be spare frequencies available to be assigned dynamically. Frequency reuse is applied when found appropriate, and where self-interference can be avoided. E.g., in Figure 1, the red and blue MANETs could be assigned with the same frequencies if the separation is sufficient to avoid interference. Thus, the DSM is in charge of the dynamic frequency coloring of MANETs. The DSM protocol should manage the spectrum resources in such a way that any interference due to mobility or external jammers is handled by algorithms that ensure the frequency hopsets are altered dynamically to avoid unreliable communication due to interference. A part of this solution is the enhanced Network Time Synchronization, that will ensure synchronization between MANETs to obtain a tighter frequency reuse. However, the main conductor is the DSM protocol, which is described in the next section.

IV. DSM Solutions for Multi-Radio MANETs

A. On Spectrum Scarcity, Coalition Cooperation, Jamming and Interference Resilience

Spectrum use can be intense in large military formations such as coalition deployments, with possibly hundreds of networks within interference reach of one another. When conventional spectrum management processes are applied, all the available VHF and UHF spectrum is often assigned to users and hence formally occupied. Still, all the spectrum is not actually used all the time. Typically, there are spectrum opportunities that can be exploited if the MANET radios can decide which spectrum to use at a given geographical location. Such local DSM is challenging in military networks, as it is also necessary to coordinate with non-communicative activities, such as electronic warfare. Therefore, compromises must be found between spectrum planning and coordination of spectrum use, and being able to swiftly adapt to the actual scenario of the operation.

Besides self-interference, there could also be adversary competing use of the VHF and UHF spectrum, as well as deliberate jamming. In recent years, much has become openly known about the volume and variety of military jammer systems that are targeted at VHF and UHF communications [26], and it is very clear that deliberate jamming must be expected. It is thus important that the VHF and UHF networks have resilience to all of the interference sources listed above, particularly including resilience to deliberate jamming. Since the military VHF and UHF networks are often used for command, control and coordination, and since digital processes and data is becoming more and more vital in military operations, this emphasizes the need for resilient networks. Several design features have been added under the hypothesis that they would contribute to such jamming and interference resilience:

(1) The use of combined VHF+UHF network radios with VHF+UHF routing may aid in routing packets around jammed areas;

(2) Important control traffic, such as DSM signaling, is sent on both the VHF and UHF bands for redundancy—the longer reach of VHF links and the higher bandwidth of the UHF links are key parameters that constitute the uncorrelated link characteristics vital for system resilience; (3) A local DSM (L-DSM) in every radio reacts fast on sudden self-interference or jamming, by adapting frequency hopping patterns on network-by-network basis with the use of a set of available frequencies, previously provided by a central DSM (C-DSM);

(4) The jamming and interference may break the connection to the C-DSM. If this occurs, the solution should continue to work using only local information;

(5) A wideband sensing entity should provide reliable information, concerning self-interference and/or external jamming.

B. Wideband Sensing

Each radio node performs multi-radio narrowband sensing in every hop and gathers the sensing results in a wideband sensing entity to give a quasi real-time representation of the VHF and UHF frequencies on which the radios are hopping. The solution can be used in military context without any significant effort from the signal processing point of view, as silent periods of synchronized VHF and UHF networks can be exploited based on the characteristics of VHF and UHF waveforms, i.e., the carrier-sense mechanism in carrier sense multiple access (CSMA) or the guard time mechanism in time division multiple access (TDMA).

In this section we first present the general model for narrowband/wideband sensing and the different test statistics along with simulation results for comparison. Then we describe three wideband sensing approaches and motivate the choice of the wideband sensing approach used by the DSM. The goal of the simulation results and figures for narrowband/wideband sensing is to provide some insights about performance, complexity and signaling overhead of different test statistics, samples vector sizes, data fusion schemes and number of channels for spectrum sensing with and without cooperation. This allows to better understand the tradeoff between performance, complexity, and reaction speed for different sensing algorithms and the choice of the wideband sensing algorithm made in the DSM design. We consider the general hypothesis testing model

$$\begin{aligned} H_0 &: Y_i = W_i \\ H_1 &: Y_i = X_i + W_i, \end{aligned} \tag{1}$$

where X_i are the received complex samples of the transmitted signal and W_i is the complex Gaussian noise. In the case of narrowband sensing, the samples Y_i are either time or frequency series of the received complex samples. In the case of wideband sensing, the samples Y_i are grouped by Nfft/NChannels frequency series (bins) of the received complex samples, Nfft being the FFT size and NChannels the number of channels. We now consider the random variable $S_i = \| Y_i \|^2$, which corresponds to the received energy.

The signal processing algorithms for wideband sensing are based on hypothesis testing. Considering a test statistic S and a threshold λ, a signal is considered absent (H_0) if the test statistic is lower than the threshold and present if the test statistic is higher than the threshold. These two hypotheses can be formulated as

$$\begin{aligned} H_0 &: S < \lambda \\ H_1 &: S > \lambda. \end{aligned} \tag{2}$$

The different test statistics considered are the energy detection (ED) statistic, the Anderson Darling (AD) statistic and the LLR-based (ZA) statistic

$$\begin{aligned} &\text{ED:} \quad S = \sum_{i=1}^{N} \| Y_i \|^2 \text{, and } \lambda = \sigma^2 \chi^{-1}\left(1 - P_{fa}, 2N\right), \\ &\text{AD:} \quad S = N - \frac{\sum_{i=1}^{N} (2i-1)(\ln F_0(X_i) + \ln(1 - F_0(X_{N+1-i})))}{N} \\ &\qquad \text{and } \lambda \text{ as in [28]}, \\ &\text{ZA:} \quad S = -\sum_{i=1}^{N} \left[\frac{\ln F_0(X_i)}{N - i + 0.5} + \frac{\ln(1 - F_0(X_i))}{i - 0.5} \right] \\ &\qquad \text{and } \lambda \text{ as in [29]}. \end{aligned} \tag{3}$$

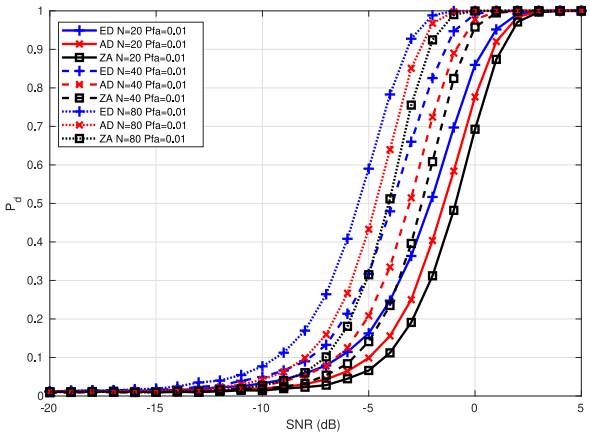

Fig. 2. Narrowband performance of ED, AD and ZA with N.

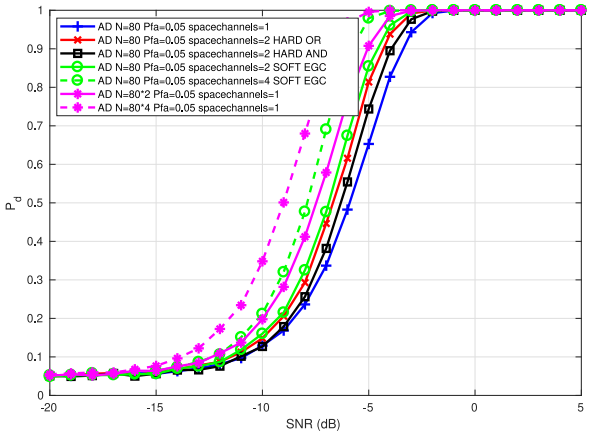

Fig. 3. Narrowband performance of cooperative AD.

Under the H_0 hypothesis, the variable S is chi-square distributed with $2N$ degrees of freedom. Data fusion schemes are also applied to the test statistics for cooperative wideband sensing [29].

Figure 2 shows the narrowband performance of ED, AD and ZA with the number of samples N and a probability of false alarm 0.05. It follows that ED>*AD*>ZA (where $>$ denotes "better than") with a gain of approximately 2 dB by doubling N.

Figure 3 shows the narrowband performance of cooperative AD with $N = 80$ and a probability of false alarm 0.05. Different levels of cooperation are evaluated: full samples knowledge, soft equal gain combining, hard OR and hard AND. It follows that cooperative full sample transmission (not realistic) $>$ soft equal gain combining $>$ hard OR $>$ hard AND.

Figure 4 shows the wideband performance of AD with different number of channels, and where the number of samples $N = 80{\cdot}$Nfft, Nfft being the FFT size and a probability of false alarm 0.05. It can be observed that P_d is decreased with the increase of number of channels because we consider a fixed number of samples and the presence of the signal on the full bandwidth. This choice allows to compare the performance between a detection per channel and a detection per bin. It follows that a detection per channel $>$ detection per bin.

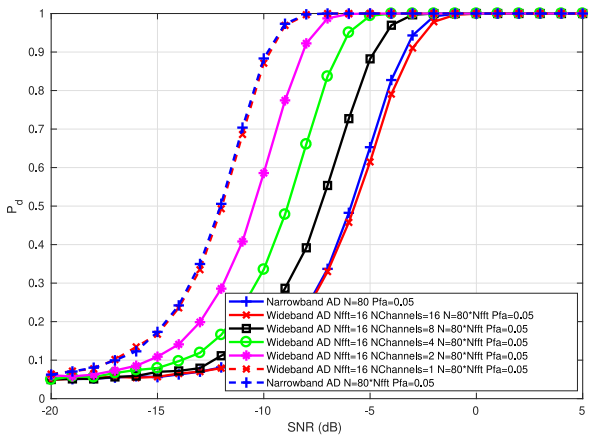

Fig. 4. Wideband performance of AD.

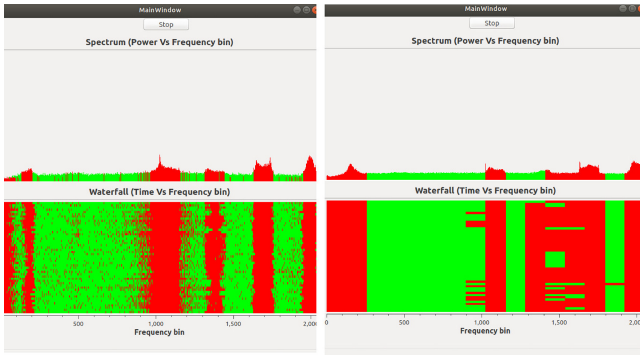

Fig. 5. Implementation of wideband AD with detection per bin (left) and detection per channel with cooperation (right).

Figure 5 shows an implementation of wideband AD with detection per bin (left) and detection per channel with cooperation using a universal software radio peripheral (USRP) B205 mini device, showing what channel can be used for transmission in green.

Several wideband sensing approaches have been evaluated with the VHF/UHF waveforms. Although for low power transmission the wideband sampling (first approach) with direct RF or direct conversion architectures is of great advantage, for military handheld radios (5W) or vehicle radios (50W), this does not work if there is another radio in the vicinity, requiring a traditional RF architecture. More research is necessary in the domain of RF architectures to have electronics capable of handling 30 dBm blockers for wide bandwidths. The second approach based on the reservation of slots of the VHF/UHF waveforms for wideband sensing requires a significant amount of time to have a representation of the VHF and UHF frequencies on which the radios are hopping and has an impact on the capacity of the VHF and UHF networks. Therefore, a third approach using silent periods in each hop of the VHF/UHF waveforms for wideband sensing is the preferred approach. This approach allows a faster representation of the VHF and UHF frequencies on which the radios are hopping and has no impact on the capacity/throughput/performance of the VHF and UHF networks.

An illustration of the solution is given in Figure 6. Each silent period (gap) of each hop is exploited to perform a

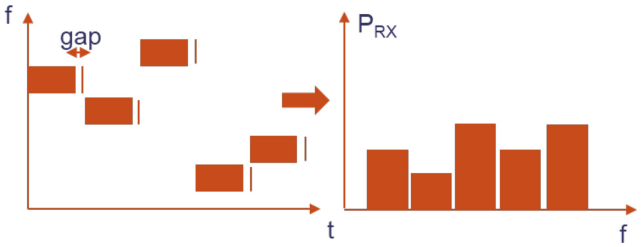

Fig. 6. Representation of wideband sensing by exploiting silent periods (gaps) in each hop.

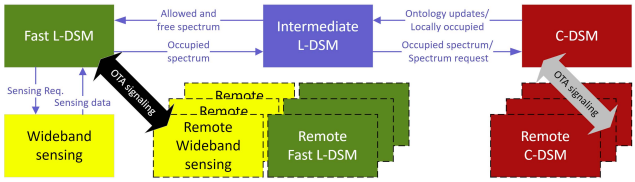

Fig. 7. The DSM architecture with three DSM entities and the wideband sensing entity. Thin arrows indicate local entity communication in each radio, while thick black or gray arrows shows OTA communication.

narrowband sensing/estimate of the noise/interference power, such that a first wideband sensing representation at the local node can be drawn after several hops and updated every hop.

The VHF waveform is based on 25 kHz STANAG NBWF, while the UHF waveform is a 1.25 MHz SC-FDMA waveform [14], [30]. With the VHF waveform, silent periods (gaps) from 2 to 5 ms already exist within its TDMA slots, which correspond to 960 or 2400 samples at 480 ksps for 2 ms or 5 ms. This amount of samples is more than enough to have an accurate detection/estimation of interference/noise power (results are given for 20-80 samples). Taking into account a hopping rate of 44 hops/s and a bandwidth of 25 kHz, at least 52 seconds are necessary to have a representation of the complete VHF spectrum 30-88 MHz if all channels are used for frequency hopping. With the UHF waveform, a silent period of 100 samples already exists within its TDMA slots. Taking into account a hopping rate of 600 hops/s, a sampling rate of 2 Msps and a bandwidth of 1.25 MHz, at least 0.23 seconds are necessary to have a representation of the complete UHF spectrum of 225-400 MHz if all channels are used for frequency hopping.

C. DSM Design

The proposed DSM architecture has three DSM entities and one wideband sensing entity, see Figure 7. These entities are present in every radio terminal to enable the distributed and robust DSM concept. In the figure, the wideband sensing entity (as explained in previous section) is shown in yellow and the central DSM (C-DSM) is shown in red. The local DSM is divided into two parts: the ''Fast L-DSM" (green) and the ''Intermediate L-DSM" (blue). Their remote counterparts, i.e., entities in other radio terminals in the network, are shown in their respective colors, but within a dashed outlined box. In short, the DSM concept is as follows:

1) The Fast L-DSM is fostered with local wideband sensing information, to enable fast reaction in case of interference (jamming or neighbor network interference).
2) To validate interference, it will also query sensing values from nearby radio terminals, using over-the-air (OTA) signaling (black thick arrow in the figure).
3) If validated, it will replace any interfered frequencies in the current hopset by selecting replacement frequencies from a set that has been provided by the Intermediate L-DSM.
4) The Intermediate L-DSM has provided this list based on available frequency spectrum given by C-DSM, and neighbor network information such as geographical positions, using ontology reasoning. Due to already conducted C-DSM OTA signaling, the list of replacement frequencies will be identical to all radio terminals belonging to the same network, and is immediately available.

The architecture is motivated by the challenges that DSM systems face in military scenarios, with possibly intermittent or broken connections to C-DSM entities, and rapidly varying local spectrum availability. Dividing the DSM into three parts enables a loose coupling between the holistic spectrum management system and the local DSM, such that fast local responses to local changes in spectrum availability are possible even without online connectivity to C-DSM. The roles and interplay of the three DSM entities are outlined more in detail in the following.

1) C-DSM: holds the information about which parts of the spectrum are available at a given location and a given time. Benefiting from Semantic Web technology, the information is in the form of an ontology ("computable conceptual model") [24], [31] in the Web Ontology Language (OWL) [32], as suggested previously in the literature [22], [24]. When there is a change to the ontology, the new ontology is sent from the top-level C-DSM to the other C-DSMs. Changes to the ontology are supposed to be infrequently needed and are therefore not included in the relatively short-duration simulations published in this paper. The ontology holds Spectrum Elements, and the information in each spectrum element includes location, frequency range, time, and spectrum access mode (e.g., open sharing or exclusive use). In the implementation in the simulator, the ontology is populated according to the spectrum resources defined available in the initialization files of the actual simulation performed, and all spectrum resources are considered available for open sharing among networks.

The C-DSM also holds a snapshot spectrum use database, that keeps track of all network's dynamics when it comes to frequency use and geographical positions, inspired by IEEE 802.22 [33]. The information is stored in a table indexed with unique communication network IDs. At local spectrum changes or radio terminal position changes (more than a given threshold, e.g., 250 meter has been used in our simulations), the Fast L-DSM informs the Intermediate L-DSM about the change and about the network's mean geographical position, and the Intermediate L-DSM relays this information to C-DSM, in order for the snapshot spectrum database to be updated. Selected "head" C-DSM radio terminals will broadcast such updates over-the-air along with network ID and

location. Due to the short-duration simulations in this paper, the snapshot spectrum database is assumed initialized at $t = 0$ of the simulation, i.e., it is assumed that at $t = 0$ the scenario has been operating long enough for the database to be fully updated. The spectrum database is then maintained with the mechanisms described above, during the simulation.

2) Intermediate L-DSM: provides "free and available channels" in a given local area. It does this by reasoning on the latest copy of the ontology [22], [24] using the Semantic Web Rule Language Application Programming Interface (SWRL API) [18], [19], to find the available channels at the current time and location. Further, it finds which of the available channels are free, by performing requests to the C-DSM spectrum use database.

3) Fast L-DSM: is responsible for the actual spectrum that is used in a network. It gets available and free frequencies from the Intermediate L-DSM, as well as sensing data from the wideband sensing entity, and performs the spectrum change if needed. The reason it is named "Fast" is because of its local access to wideband sensing, and to Intermediate L-DSM and C-DSM information, as shown in the upper part of Fig. 7. This information is sufficient to perform short-term frequency assignment adjustments to address detected jamming or other frequency conflicts. Its OTA signaling consists of

1) $\mathrm{req}(f, L_l)$: request for remote sensing level on frequency *f*, local level is L_l,
2) $\mathrm{resp}(f, L_r)$: response with sensing level L_r on frequency *f*, and
3) $\mathrm{fch}(f_{old}, f_{new}, t)$: replace the use of f_{old} with f_{new} at time *t*,

all being broadcast messages, where the two first messages constitutes the cooperative sensing part. The broadcasted cooperative sensing request is satisfied upon the first $\mathrm{resp}(f, L_r)$ reply that confirms the anomaly, which typically is provided from one of its closest one-hop radio node neighbors. The OTA messages are explained more at the end of this subsection.

The core algorithm [34] of Fast L-DSM is based on the well known Satisfaction Equilibrium [15] principle, where the goal is to converge to a state where "all agents are satisfied by their payoff under their satisfaction function and do not need to change their strategy when they are satisfied" [15]. The algorithm has a built-in geographical priority resolution mechanism to solve DSM spectrum conflicts between communication networks.

In the following, C_i is the hopset used by the communication network entity *i*, consisting of one or more individual channels c_k. Ω is the set of *M* available channels (or spectrum segments) received from the local intermediate DSM module. $\Psi_{\setminus i}$ is the set of all communication network entities, not including *i*, that are within interference range of entity *i*. $\Psi_{W\setminus i}$ is the set of all communication network entities, not including *i*, that are within interference range of entity *i* and that are positioned to the west of *i*. We denote $\Psi_{X\setminus i} = \Psi_{W\setminus i}$ if location data for the communication networks are known, otherwise $\Psi_{X\setminus i} = \Psi_{\setminus i}$. The west direction has been chosen arbitrarily as a geographical priority resolution criterion. If location data is known, only networks within interference distance to the west are considered as interference, and the frequencies used in eastbound networks are assumed available. The motivation is that, over time and with reliable detection of interference, spectrum conflicts should migrate towards the east, to get resolved in areas where spectrum use is less dense.

The subset of channels that are in use as seen from the communication network *i* is $\hat{\Omega}$,

$$\hat{\Omega} = \bigcup_{j \in \Psi_{X\setminus i}} C_j, \tag{4}$$

and the available channels that are not used by other networks within interference range are

$$\bar{\Omega} = \Omega \setminus \hat{\Omega}. \tag{5}$$

When there is a need to modify the current hopset, the set of channels from which the new channel in the hopset is selected from is

$$\tilde{\Omega} = \bar{\Omega} \setminus C_i. \tag{6}$$

In the implementation in the simulator, the Fast L-DSM detects the need for hopset change, and assesses the possibility for hopset C_i modifications, if at least one of these two situations occur:

1) Its local wideband sensing entity reports unusual high noise levels, or
2) An incoming control message from a remote Fast L-DSM entity instructs it to act.

In case i), and only a single or a small portion of the used spectrum reports such noise levels, the radio will broadcast a message $\mathrm{req}(f, L_l)$ requesting any receiving radios within the MANET to respond with $\mathrm{resp}(f, L_r)$ showing its noise levels L_r on the indicated frequency f. By confirming at least one other node to detect the presence of an interferer, cooperative spectrum sensing is considered with HARD AND, at least 2 space channels and different SNRs similar to the black line on Figure 3. This approach allows to increase reaction speed, to broadcast messages with minimum payload and to reduce the probability of false alarms due to self-interference. If any response is confirming a value L_r above threshold, the Fast L-DSM will proceed to calculate a modified hopset, and to share this information using OTA broadcast signaling. This "Change current hopset frequencies" message $\mathrm{fch}(f_{old}, f_{new}, t)$ includes old and new frequencies, as well as the time of change. The time for change is selected with some latency, to allow all radios to receive the control message prior to this time instant. In case all radio nodes *n* sense the spectrum jamming simultaneously, and all receive the $n - 1$ number of $\mathrm{req}(f, L_l)$ broadcast messages, the network will experience a flooding of $n(n-1)$ number of $\mathrm{resp}(f, L_r)$ messages. To constrain this response traffic volume, we have implemented a functionality that creates a time window that ensures remote sensing replies only occur once per node per new $\mathrm{req}(f, L_l)$ event, i.e., the "complexity" of this traffic volume should reach a scaling of $\mathcal{O}(n)$ instead of $\mathcal{O}(n^2)$.

In case i), and a large part of the used spectrum reports such noise levels, the radio terminal will conclude that Fast L-DSM operations must take place, without asking remote radios for confirmation. The rationale for this is to increase

the probability of successful jamming mitigation when the spectrum is severely affected.

4) DSM Entities Interplay: When the Fast L-DSM has decided it needs to replace one or more frequencies in the hopset, it will get the frequency candidate list of "free and available channels" from the Intermediate L-DSM, by supplying to the Intermediate L-DSM the radius of the considered interference range as well as a Boolean "Siderule" parameter. When the "Siderule" parameter is true, only occupied channels from set $\Psi_{W\setminus i}$ are considered when calculating free spectrum, while $\Psi_{\setminus i}$ is considered if this parameter is false.

Using the list of "free and available frequencies", the selection of a replacement frequency is performed totally distributed by each radio, by seeding its pseudo random engine with the index of the affected interfered frequency. Since all radio terminals belonging to the same MANET will generate the same list of possible new frequencies, they will all select the same replace frequency. Only in the case of wideband jamming this condition may be broken, since the terminals might not detect all affected frequencies in the same detection event. To tackle such situations, a conflict resolution algorithm is included with a mitigation strategy to always accept the lowest replacement frequency suggestion. This strategy also accepts to delete a frequency completely, in case the list of available replace frequencies has been emptied. The rationale in having a distributed replacement frequency algorithm is to speed the reaction time, and being completely dynamic in constructing updated hopsets.

When a MANET is severely interfered, reliable control signaling can be compromised, and this makes it challenging to ensure that all radios that belong to this MANET will change to a modified hopset simultaneously. A way to alleviate this situation is to utilize overlapping geographical coverage of different MANETs. As an example, a long range VHF network can act as an "umbrella" network to broadcast the selected UHF control messages. This resilience is indeed exploited and shown demonstrated in our simulations, see, e.g., Section VII-A.

V. Network Time Synchronization

At the individual network level, network time synchronization (NTS) is essential for time synchronous communication schemes such as time division multiple access. It is also essential for maintaining orthogonal frequency hopping patterns among networks. This calls for inter-network NTS and could be called Extended NTS (ENTS). It increases overall robustness and can deliver the best available NTS timing source to different networks, e.g., a time from a global navigation satellite system (GNSS) if that is available. Details of the developed, generic ENTS algorithm can be found in [12]. Herein, the main principles are given.

ENTS is an entity that is active in the multi-radio terminals. It takes NTS time information from the NTS algorithms in individual networks, decides which time will be used, and shares this information to all networks. Since this time is an external master time to the networks, the NTS algorithms must be capable of taking the external master time source. Otherwise, the individual NTS algorithms are not touched. ENTS should be aware of NTS requirements in individual waveforms, such that it does not force them to use a too loose time source. It applies policies set by end users. An example policy is that a GNSS time must be used if available, except if it does not violate the accuracy requirements, which may occur if the GNSS time is delivered from a distant narrowband system.

VI. Routing Protocol Solutions

A. The Routing Protocol

The Upper NET enables dynamic routing between terminals in different MANETs. The routing solutions use a two-layer approach where the Upper NET layer is responsible for routing between the MANETs while the Lower NET layer is responsible for the MANET internal routing. The Upper NET sees all radios that are reachable by a MANET, via the MANETs internal routing, as one-hop neighbors. Hence, a link in the Upper NET can correspond to a multi hop route in the Lower NET. The routing daemon of the Upper NET is based on a modified version of OLSR (Optimized Link State Routing protocol), as described in [35].

The aim of the modifications is to reduce the amount of control traffic introduced by the Upper NET by utilizing (i) the Lower NETs capability of broadcasting packets to all radios reachable in a MANET and (ii) the topology information collected by the Lower NETs. The modifications include improved Multipoint Relay (MPR) forwarding rules, compressed control messages, link information from the Lower NET, reactive Hello and TC (traffic control) messages, and link cost aware routing. The additions are further described below:

1) Improved MPR Forwarding Rules: Given the Lower NETs capability of broadcasting packets to all radios reachable in a MANET, the MPR in the Upper NET never retransmits a packet to the receiving interface.

2) Compressed Control Messages: A hybrid compression method is used that combines the vector approach from [35] with the (24-bit) prefix approach in [36], so that the best of the two methods is selected packet by packet. Furthermore, the header of the prefix method is reduced compared to the method described in [36], since only network prefixes are supported.

3) Link Information From the Lower NET: The detection of links at the Upper NET layer is based solely on information from the Lower NET layer. Links and associated neighbors are removed immediately when the corresponding link is detected as broken.

4) Reactive Hello and TC Messages: When cross-layer information is available, there is no need to send Hello messages to discover links. Hence, a Hello interval of 512 seconds is used, combined with reactive Hello messages that are sent on link and MPR updates. As in the OLSR standard, TC messages are sent in a reactive manner when changes in the MPR selection set occurs. The TC interval is increased to 60 seconds, at the expense of a possibly slower network merging. However, this is more or less avoided by using the TC message inspection method [35]. To further increase

the robustness, additional control messages are sent after the initial reactively triggered message. It is done in accordance with [35], with a delay of two and five seconds for the first Hello and TC messages, respectively. To limit the amount of control messages, the interval between messages of the same type is at least two seconds.

5) Link Cost Aware Routing: The algorithm is modified so that costs can be associated to the links in the Upper NET. The cost is set to one for UHF and to 40 for VHF. Furthermore, the shortest-path algorithm is replaced by an implementation of Dijkstra's algorithm [36].

In addition to the described changes, it is assumed that the main address and interface addresses for each radio are assigned by a predefined address plan. Hence, the Multiple Interface Declaration (MID) messages are replaced by a parse of the address plan during terminal initialization.

B. The Interplay of DSM and Routing

When a MANET, or a part of a MANET, experiences excess number of packet drops due to interference, the architecture with Upper NET and DSM has two measures to resolve the situation. E.g., assume that the green MANET in Figure 1 is severely affected by an external jammer, and that user A can no longer communicate with user D. If there exists a fourth MANET, located just south of the green MANET and that could be used as a bridge between the red and the blue MANET, the Upper NET should react to establish this rerouting. Simultaneously, the DSM entities have started to mitigate the infected part of the spectrum, and in the case there are enough free and available frequencies, a healed green MANET can be provided. While these redundant mitigation activities serve increased robustness, they can also pose some challenges due to increased OTA control traffic. Especially, for the narrow bandwidth VHF MANETs this issue was revealed problematic, and measures were implemented to be as traffic load conservative as possible without sacrificing functionality performance.

In the Fast L-DSM entity, a functionality named Quality Parameter Function (QPF) was defined that should serve spectrum and DSM information to the Upper NET. The following list of functionalities was assessed: (i) Interference levels and jamming situation in the two bands, (ii) Likelihood of receiving enough transmission resources, (iii) Link stability, (iv) Traffic congestion further away in the network, (v) Queue fill, and (vi) C-DSM information about planned forthcoming changes in the military theater. E.g., in (i), the Upper NET could utilize the message "severe interference in network Nx ongoing" to apply smarter routing protocol activities than without this information. The functionality Adaptive Link Selection (ALS) was defined in Upper NET to handle this kind of supplied information. Up to now, only option (i) has been implemented in the simulator, where the ALS saves a locked version of the routing table of the affected MANET air interface in the period when this interface is in jammed state. When the DSM has mitigated a jamming, or a jamming stops, the saved routing table will be reinserted, enabling a significant faster reschedule of packet forwarding through Upper NET.

TABLE I
SIMULATIONS OVERVIEW AND KEY SPECTRUM METRICS (FREE FREQUENCIES GIVEN ARE THE COUNTS AT $t = 0$)

Sim. scenario (section)	# of seeds	UHF freqs. assigned	VHF freqs. assigned	UHF/VHF Tx power (W)	UHF/VHF jammer power (W)
A.	10	17 (1 free)	16 (8 free)	20/10	25/25
B.	9	12 (7 free)	5 (0 free)	2/5	50/–
C.	8	48 (20 free)	1620 (50% free)	50/50	100/50

VII. SIMULATION RESULTS AND DISCUSSIONS

In the MAENA project, the MANETs investigated were using VHF and UHF frequency hopping waveforms with a hopset size of 3–12 physical frequencies. As already mentioned, the VHF waveform was based on 25 kHz STANAG NBWF (narrow-band waveform), while the UHF waveform was a 1.25 MHz SC-FDMA waveform [14], [30]. Together with our DSM, routing, and network synchronization designs, these waveforms were implemented into the "MAENA simulator". The simulator engine was based on OMNEST (the commercial version of OMNET++ framework), including a tailored network scenario definition tool (a graphical Human-Machine Interface that defines XML code, and translated to OMNEST.ini files when parsed), and a performance metric database with dedicated visualization tools. This resulting simulator is not a conventional event based network simulator, since it also includes the PHY layer with channel coding and modulation I/Q sample waveform details. In addition, it includes large and small-scale fading modeling, co-site interference, and path loss calculation using digital terrain maps. These features come at a cost of increase in CPU load and time of simulation experiments, but produce results with much improved credibility.

In the following, some simulation results are given, to demonstrate the performance of our DSM and routing architecture in three different challenging network scenarios (see overview of key spectrum parameters in Table I). As a common challenge of these scenarios, all the UDP/IP flows bit rates are much higher than the VHF networks capacities, typically 40 kbit/s. The VHF networks are, however, capable of relaying UHF network signaling traffic, to assist both the DSM and routing protocols.

A. DSM/Routing Testing in Small-to-Larger Scenario

The main purpose of testing this network was to validate the DSM and routing capabilities with radios having up to four air interfaces, and that interfered frequencies in both VHF and UHF networks could be mitigated using signaling in both VHF and UHF networks. Additionally, the scenario should unmask the performance effect of DSM Siderule and ALS, and how the user data delivery performs and signaling overhead grows with the number of radio nodes in the networks. We included scenarios with five, 10, and 20 radios in this investigation.

The presented scenario in Figure 8 displays the smallest network, for explanation simplicity, with only five radios (R1–R5), three UHF networks, and one VHF network. (The two larger scenarios have the same area and number of UHF

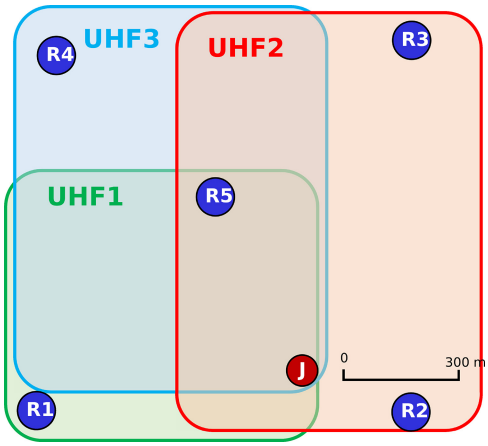

Fig. 8. The small scenario has 5 radios (Rx) and one jammer (J). There are 3 UHF networks and one "umbrella" VHF network (including all five radios).

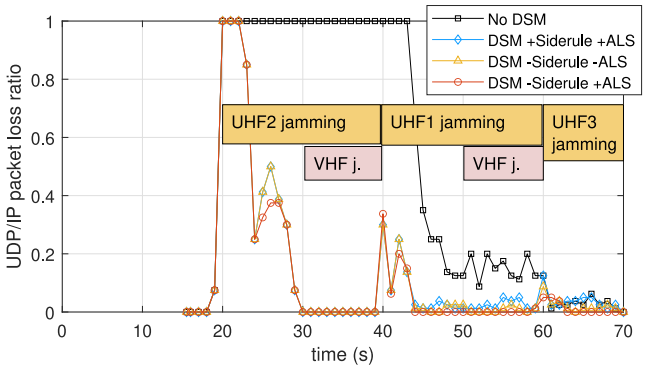

Fig. 9. Sequential jamming – UDP/IP packet loss ratio maximums from all five flows, in four different DSM cases: No DSM, and DSM with three combinations of Siderule and ALS (+=on, −=off).

and VHF networks, the same UDP traffic, but where the density of radio nodes are increased.) R5 is serving as a gateway between all UHF networks, since it has 3 UHF (and 1 VHF) air interfaces. The other radios have one VHF and one UHF air interface. There are five UDP/IP flows lasting from 15 until 70 s:

1) R1 to R2 via R5, (UHF1 and UHF2)
2) R2 to R3, (UHF2 only)
3) R3 to R4 via R5, (UHF2 and UHF3)
4) R4 to R5, (UHF3 only) and
5) R5 to R1, (UHF1 only)

all with a bit rate 40 kbit/s each. UHF2 is jammed at 20–40 s, UHF1 at 40–60 s, and UHF3 at 60–70 s. The VHF network is jammed at 30–40 and 50–60 s.

Figure 9 shows the average packet loss ratio of all flows (and all seeds) in four different cases. The black line shows the loss when the DSM mechanism is disabled, i.e., the conventional frequency management reference case. The UHF2 jammer is active between 20 and 40 seconds, and its position gives a significant influence on the performance of the flows R1-R5-R2 and R2-R3. Due to longer range between the jammer and the affected radios in the 2nd and 3rd jamming events, these losses are more restricted, even without DSM activated.

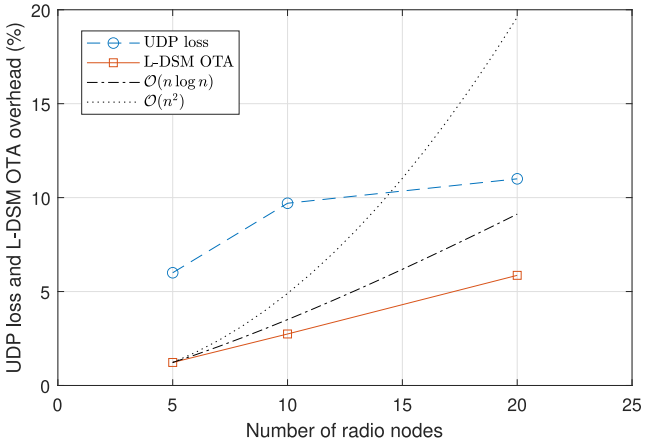

Fig. 10. The L-DSM overhead traffic shows linear scalability, while UDP loss rate is constrained (all results averaged over time and 10 different seeds).

The blue line shows the loss ratio when DSM is activated with the Siderule and ALS functionality. The 1st DSM jamming mitigation is completed around 24 seconds, but due to independent operations between routing protocols of Lower NET and Upper NET, it often experiences a second phase of packet losses between 26–28 s. Due to the Siderule only the eastern UHF2 DSM is taking into consideration other UHF MANET spectrum use, the activated replace frequencies of UHF1 (at 44.0 s) and UHF3 (at 64.0 s) might interfere with UHF2. This causes the residual packet loss events seen.

The red line shows the loss ratio when the Siderule functionality is off (but ALS on), which make the UHF networks to consider all their neighbor networks' spectrum use. As seen, after jamming mitigation, further packet losses are totally absent. The results are inline with our design goals, since also the number of spare frequencies were sufficient in establishing orthogonality between the neighbor networks. The yellow line shows the poorer results when ALS is off, and reveals the size of its positive contributions in this setup.

The larger scenarios with 10 and 20 radio nodes were simulated using the same radio parameters and jammers, but where the objective was to investigate how the L-DSM OTA signaling traffic scaled with the increased radio density. This OTA signaling traffic was normalized to the UDP user traffic volume (five flows of 40 kbit/s bit rate as before). The results presented in Fig. 10 shows that the amount of signaling traffic is scaling close to $\mathcal{O}(n)$. This is compared to $\mathcal{O}(n^2)$ normalized to the overhead value of the smallest network. This verifies that the cooperative sensing broadcasting $\mathrm{resp}(f, L_r)$ of spectrum anomaly detection are avoiding the $n(n-1)$ flooding, as designed and described in Section IV-C3. The "L-DSM OTA" line in Fig. 10 includes the traffic volume aggregated over all $\mathrm{req}(f, L_l)$, $\mathrm{resp}(f, L_r)$, and $\mathrm{fch}(f_{old}, f_{new}, t)$ messages transmitted during the simulation time. The figure also shows the aggregate reception performance of all five UDP flows. Since only R5 is interfaced to all three UHF networks, it becomes key to this performance. With the scenarios' three UHF jamming events, a UDP loss of 11.8% for network size 20 is satisfactory, especially when compared to the two smaller network sizes. Not shown in the figure is that the speed of frequency replacement does not vary with n, as the spectrum

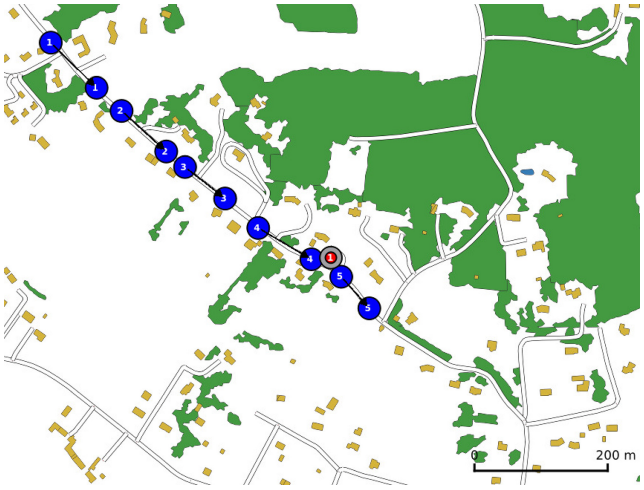

Fig. 11. The radio terminal 1–5 locations with their movements, and the wideband jammer location (red circle).

anomaly is confirmed when the first $\mathrm{resp}(f, L_r)$ arrives with L_r above threshold.

B. Wideband Frequency Jamming

In the next scenario, five mobile VHF+UHF radios (R1–R5) are moving along a road at a speed of approximately 10 km/h, see Fig. 11.

There is a wideband UHF jammer located just beside the road as they are passing, and there are four UDP/IP packet flows between a subset of the radios:

1) R1 to R4,
2) R2 to R4,
3) R3 to R1, and
4) R4 to R1.

A hopset of five frequencies is used in the UHF network, and the jammer starts emitting power on all these frequencies starting at 20 s. The latter is observed in Fig. 12 as five black lines. The DSM algorithm is started by sensed jamming levels above threshold at terminals R4 and R5, and all radios change all frequencies independently and equally, starting at approximately 23.5 s. This fast reaction is achieved partly because of the special detection of *wideband* frequency jamming: as mentioned before, the DSM algorithm skips the OTA handshake signaling requesting for remote sensing values. When R4 and R5 plan their frequency change, they inform that this is already decided, and signals this in one-way OTA command. The receiving terminals (R1–R3) obey this command. Figure 13 shows that the 4 UDP flows experience packet losses (averaged over 9 runs) between 20–23.5 seconds, but after that the packet loss decays fast to zero.

C. Frequency Jamming of Companies and Platoons in Large Operational Scenario

In order to validate the DSM and routing algorithms in larger operational scenarios, a multi-company scenario was implemented, consisting of 157 radios divided into 6 companies and 19 platoons. Four of these companies, Company 1–4, have their own dedicated UHF network named UHF_A,

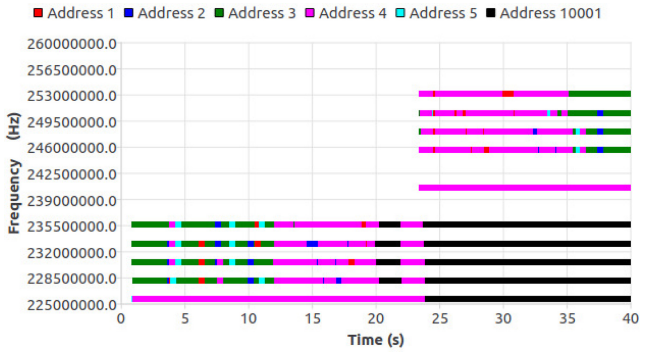

Fig. 12. Transmitter activity all radios in UHF band — the wideband jammer (address 10001) starts at 20 s, and new frequency hopset is ready and in use at approximately 23.5 s.

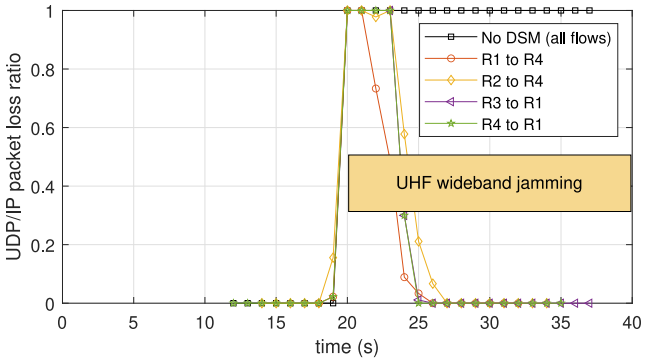

Fig. 13. Wideband jamming — UDP/IP packet losses decline fast to zero in period 23.5–26 s due to the DSM jamming mitigation success. When DSM is disabled, the packet loss is 100 % for all flows.

_B, _C, and _D, as well as Company VHF networks named Cmp1–Cmp4, respectively. Each of these company terminals are also attached to one of three platoon VHF networks, e.g., Company 4 terminals are connected to either Plt_4_1, Plt_4_2, or Plt_4_3. In addition, there is a UHF_F network which members are a sub-selection of members from Company 1–4: this ensures a possible all-UHF route path for IP flows between different companies. Each VHF network uses 10 frequencies and each UHF network uses 4 frequencies in their hopsets, respectively. There are 19 spare UHF frequencies in the scenario. Both VHF and UHF air interfaces transmit with 50 W power.

In the following investigation, the focus will be on the statistical performance of 11 UDP/IP flows where the source or the destination (or both) are inside Company 4. Table II gives an overview of these 11 flows: which terminals they are between (column 2), which networks these terminals are connected to (column 3–6), and the distance between source and destination and the distance between the UHF jammer and the destination terminal (column 7).

In this scenario there is one UHF jammer and one VHF jammer. Their positions are shown in Fig. 14 together with the radio terminal positions. The UHF jammer interfere one single frequency used in Company 4 UHF_D hopset (UHF_D radio positions are colored red in Fig. 14 and Fig. 15). The VHF jammer interfere two frequencies in each of Plt_4_1, Plt_4_2, and Plt_4_3 hopsets, i.e., 6 VHF frequencies in total.

TABLE II
LARGE OPERATIONAL SCENARIO — DETAILED AVERAGED RESULTS (UDP/IP FLOWS PACKET LOSS, E2E DELAY AND NUMBER OF HOPS)

UDP/IP		Radio node air interface network connection				Dist. (m) Tx–Rx	Expected loss, vs. simulated loss			Exp. #of hops sim. #of hops		Expected delay, vs. simulated delay (s)		
Flow #	Src — Dst	AirInt 1 (all VHF)	AirInt 2 (all VHF)	AirInt 3 (all UHF)	AirInt 4 (VHF/UHF)	Dist. (m) Rx–jammer	No DSM	Side-rule	No Side-rule	No DSM	DSM	No DSM	Side-rule	No Side-rule
1	77	Cmp4	Plt_4_1	UHF_D	-	1027.8	high	low	low	low	low	high	low	low
	89	Cmp4	Plt_4_2	UHF_D	-	722.1	87%	0-20%	0-5%	1.6	1.8	6.0	0.8	0.8
2	81	Cmp4	Plt_4_1	UHF_D	-	4847.7	high	medium	medium	high	high	high	?	?
	10	Cmp1	Plt_1_1	UHF_A	-	4601.3	81%	10-25%	0-25%	6.0	4.8	4.0	1.8	1.8
3	85	Cmp4	Plt_4_2	UHF_D	VHF_Data	301.8	high	low	low	low	low	high	low	low
	86	Cmp4	Plt_4_2	UHF_D	UHF_F	601.4	1.0%	0%	0%	1	1	0.35	0.14	0.14
4	86	Cmp4	Plt_4_2	UHF_D	UHF_F	715.4	high	low	low	low	low	high	low	low
	95	Cmp4	Plt_4_3	UHF_D	-	184.2	98%	0%	0%	2.5	2.1	12	0.8	0.8
5	87*)	Cmp4	Plt_4_2	UHF_D	-	923.3	high	low	low	low	low	high	low	low
	89	Cmp4	Plt_4_2	UHF_D	-	722.1	53%	0-5%	0-5%	1	1	6	0.55	0.55
6	91	Cmp4	Plt_4_2	UHF_D	VHF_Data	118.7	high	low	low	low	low	high	low	low
	92	Cmp4	Plt_4_3	UHF_D	UHF_F	516.5	0%	0%	0%	1.1	1	2.1	0.25	0.25
7	91	Cmp4	Plt_4_3	UHF_D	VHF_Data	432.4	high	low	low	low	low	high	low	low
	79	Cmp4	Plt_4_1	UHF_D	MrtFireCtrl	272.5	25%	0%	0%	2	2	7	0.45	0.5
8	92	Cmp4	Plt_4_3	UHF_D	UHF_F	5565.9	low	low	low	low	low	low	low	low
	1	BtlCmd	Cmp1	UHF_A	UHF_F	5080.6	0%	0-10%	0%	1.8	1.8	1.6	2	1.6
9	93*)	Cmp4	Plt_4_3	UHF_D	-	849.0	high	low	low	low	low	high	low	low
	96	Cmp4	Plt_4_3	UHF_D	-	485.5	51%	0%	0%	1	1	6	0.15	0.15
10	57	Cmp3	Plt_3_1	UHF_C	-	5507.0	high	medium	medium	high	high	high	low	low
	82	Cmp4	Plt_4_1	UHF_D	-	401.8	100%	10-20%	0-15%	6	5.5	7	1.8	1.8
11	62	Cmp3	Plt_3_2	UHF_C	UHF_F	5156.2	low	low	low	low	low	low	low	low
	86	Cmp4	Plt_4_2	UHF_D	UHF_F	601.4	0%	12%	0-12%	1.3	1.2	2	2.2	2.1

*) 160 kbit/s flow, the rest is 40 kbit/s flows

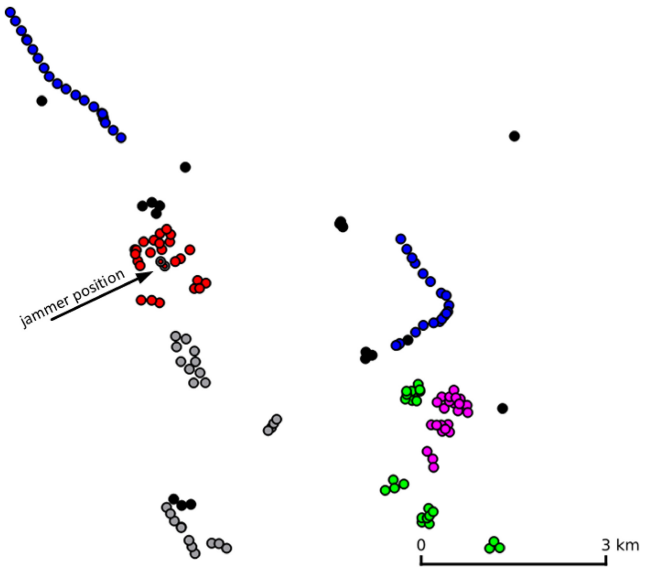

Fig. 14. The operational scenario has 157 radios in total. The two jammers (see their co-location pointed to by the arrow) interfere some frequencies used in Company 4 (the 22 nodes in red color) hopsets.

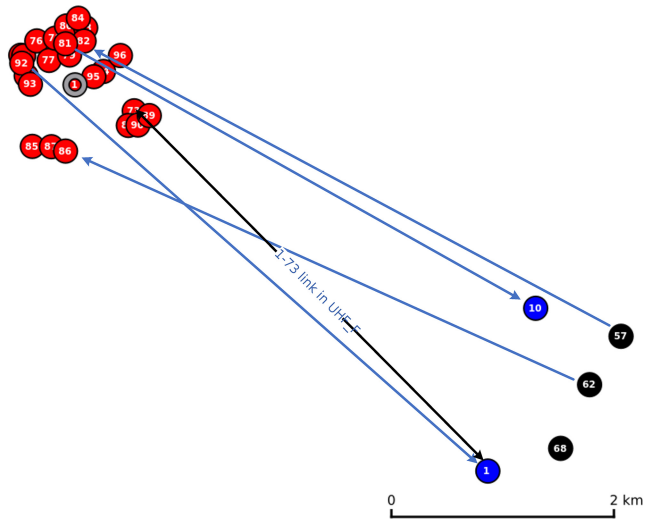

Fig. 15. Four of the UDP/IP flows are shown here, as they communicate between Company 4 and Company 1 or 3. The UHF_F network's shortest possible link is shown in black (4.5 km). All UHF_D radios are shown (red), but only a subset of the other UHF networks. The UHF jammer is located in the center of UHF_D with a small "1" inside a circle.

The VHF and UHF jamming lasts from 35.0 s until simulation ends at 100.0 s. The 11 UDP/IP traffic flows all start at 40.0 s and end at 90.0 s. This means that if the DSM system can mitigate the damage within 5.0 s the UDP/IP statistics should show losses close to zero. In Table II we have also included cells to show the *expected* results of each flow in applying DSM or not. This is based on (i) the inspection of available connected networks of the sender and receiver terminals, and (ii) the knowledge of that the jamming will result in, if no DSM, malfunction of networks UHF_D, Plt_4_1, Plt_4_2, and Plt_4_3. In case DSM is available, the expectation is that these four networks are fully recovered before the UDP/IP flows start. These expectations are labelled either "high", "medium", or "low". The averaged simulation results (eight different seeds simulated) are shown in the respective cell below.

When reading the simulation result statistics of Table II, the following main observations are made:

1) Flows 1, 2, 4, 5, 9, and 10 suffer badly in UDP packet loss when DSM is not available. The DSM solutions are able to produce either zero loss or a small

TABLE III
LARGE OPERATIONAL SCENARIO — UDP LOSS RATES (%)

Simulation run #	No DSM	DSM +Siderule +ALS	DSM -Siderule +ALS
1	16.8	0.9	0.0
2	19.8	1.3	1.3
3	15.0	1.2	1.3
4	18.3	7.8	1.1
5	16.9	0.0	0.8
6	16.7	1.1	1.2
7	16.9	1.6	1.8
8	15.5	1.1	1.0
Average	17.0	1.9	1.1

percentage of packet loss. For some flows, e.g., flow 2, the different simulation seeds provided largely different results, indicated with a range of percentage packet loss instead of a single average value.

2) Flow 3 sees almost no loss, even without DSM. The reason is that the Tx–Rx distance is small, and only half the distance to the jammer. Similar, flow 6 has the same or even better conditions.
3) Flows 8 and 11 are managed well without DSM, due to the connection to the UHF_F network. As seen, the simulation with DSM could result in somewhat worse conditions, most likely due to the added signaling traffic competing for network resources.
4) DSM with Siderule enabled has marginally slightly more loss than with Siderule disabled. The reason is due to the aforementioned issue, that the frequency replacement mitigation might select frequencies already occupied by networks to the east of the jammed network.
5) Flows 2 and 10 exhibit a high number of hops before reaching the destination. The source/destination terminal pair does not share any common network, and the flows are routed via VHF networks to reach the common UHF_F network to interconnect. The introduction of DSM with ALS reduces the number of hops and end-to-end delay significantly.

In Table III the overall UDP/IP loss statistics for the total of 45 flows (between all radios in the scenario) are shown. As seen, with DSM the packet loss statistics are reduced from 17 % to 1.9 % and 1.1 % on average with and without Siderule enabled, respectively. This is very close to our design goal of zero loss. It can be concluded that the mitigation provided by DSM and routing works as desired, even when applied in an up-scaled large network-of-networks scenario.

D. Simulation Results Wrap-Up

The simulation results show that both the DSM and routing entities are working, and that their algorithms create significantly improved results compared to when DSM is not activated (Figures 9 and 13, and Table II and III). The interfered frequencies are replaced by non-interfered frequencies (Fig. 12), and the Upper NET ensures that packet forwarding is resumed when the link is repaired by DSM or another route is found. Table II shows that the solution works efficiently in large scenarios, including many VHF and UHF networks.

VIII. CONCLUSION

This paper has presented the architecture and performance of a collaborative DSM and Upper NET protocol that was developed in the MAENA project for its use in military VHF and UHF ad-hoc networks. The utilized VHF and UHF waveforms also benefit from network time synchronization functionality to assist orthogonality between neighbor networks. It has been shown that both narrowband and wideband frequency jamming can be mitigated after just 3–5 seconds, and packet forwarding resumed shortly after. The architecture also showed good scaling performance in that a large operational scenario was simulated with 157 radio terminals serving 6 companies and 19 platoons. Here, the overall packet losses in 45 UDP/IP flows were reduced from 17 % to 1.1 %. When studying the 11 UDP/IP flows that directly suffered from jamming, many flows experienced dramatic reduction of packet losses when DSM was enabled, such as from 98 % to 0 %. We find this as solid validation that the design goals of the proposed DSM architecture have been accomplished.

REFERENCES

[1] I. F. Akyildiz, W.-Y. Lee, M. C. Vuran, and S. Mohanty, "A survey on spectrum management in cognitive radio networks," *IEEE Commun. Mag.*, vol. 46, no. 4, pp. 40–48, Apr. 2008.

[2] "Cognitive radio networks: efficient solutions for routing, topology control, data transport, and network management," NATO STO, Brussels, Belgium, Tech. Rep. IST-140, 2019.

[3] J. L. Burbank, P. F. Chimento, B. K. Haberman, and W. T. Kasch, "Key challenges of military tactical networking and the elusive promise of MANET technology," *IEEE Commun. Mag.*, vol. 44, no. 11, pp. 39–45, Nov. 2006.

[4] "Heterogeneous tactical networks–Improving connectivity and network efficiency," NATO STO, Brussels, Belgium, Rep. IST-124, 2019.

[5] J. Mitola, "Cognitive radio: Model-based competence for software radios," in *Tekniska högskolan i Stockholm Institutionen för Teleinformatik D* (Trita-IT: AVH). Stockholm, Sweden: KTH, 1999. [Online]. Available: https://books.google. no/books?id=9DEAjwEACAAJ

[6] M. Buddhikot, P. Kolodzy, S. Miller, K. Ryan, and J. Evans, "DIMSUMNet: New directions in wireless networking using coordinated dynamic spectrum access," in *Proc. 6th IEEE Int. Symp. World Wireless Mobile Multimedia Netw.*, 2005, pp. 78–85. [Online]. Available: http://ieeexplore.ieee.org/document/1443488/

[7] P. Flavell, P. Adams, G. Capela, and L. Bastos, "Adopting a dynamic spectrum management philosophy in NATO," in *Proc. IEEE Mil. Commun. Conf. (MILCOM)*, 2021, pp. 366–371.

[8] J. Lopatka, T. Paso, R. Massin, and X. Leturc, "Multi band efficient networks for ad hoc communications," *Procedia Comput. Sci.*, vol. 205, pp. 88–96, Jan. 2022. [Online]. Available: https://linkinghub.elsevier.com/retrieve/pii/S1877050922008754

[9] P. Gajewski, J. Lopatka, and P. Lubkowski, "Traffic modelling for mobile ad-hoc networks simulation," in *Proc. Signal Process. Symp. (SPSympo)*, Sep. 2021, pp. 70–75. [Online]. Available: https://ieeexplore.ieee.org/document/9593720/

[10] X. Leturc, E. Janin, and C. J. le Martret, "Distributed dynamic channel assignment in military ad hoc networks within the maena project: New algorithm and high fidelity simulation results," in *Proc. IEEE Mil. Commun. Conf. (MILCOM)*, San Diego, CA, USA, Nov. 2021, pp. 945–950. [Online]. Available: https://ieeexplore.ieee.org/document/9653046/

[11] P. Skokowski, K. Malon, and J. Łopatka, "Building the electromagnetic situation awareness in manet cognitive radio networks for urban areas," *Sensors*, vol. 22, no. 3, p. 716, 2022. [Online]. Available: https://www.mdpi.com/1424-8220/22/3/716

[12] H. Saarnisaari, J. Markkula, T. Paso, and T. Bräysy, "Internetwork time synchronization of mobile ad hoc networks," *IEEE Access*, vol. 9, pp. 84191–84203, 2021.

[13] K. Malon, J. Łopatka, and P. Skokowski, "*Q*-learning based radio channels utility evaluation algorithm for the local dynamic spectrum management in mobile ad-hoc networks," in *Proc. Baltic URSI Symp. (URSI)*, 2020, pp. 28–32.

[14] L. Rose, R. Massin, L. Vijayandran, M. Debbah, and C. J. Le Martret, "CORASMA program on cognitive radio for tactical networks: High fidelity simulator and first results on dynamic frequency allocation," in *Proc. IEEE Mil. Commun. Conf. (MILCOM)*, 2013, pp. 360–368.

[15] S. Ross and B. Chaib-draa, "Satisfaction equilibrium: Achieving cooperation in incomplete information games," in *Advances in Artificial Intelligence*, L. Lamontagne and M. Marchand, Eds. Berlin, Germany: Springer-Verlag, 2006, pp. 61–72.

[16] B. Ellingsæter, "Frequency allocation game in satisfaction form," *Trans. Emerg. Telecommun. Technol.*, vol. 25, no. 12, pp. 1238–1251, 2014.

[17] "Web ontology language." 2013. Accessed: Jan. 25, 2022. [Online]. Available: https://www.w3.org/2001/sw/wiki/OWL

[18] M. O'Connor, R. Shankar, M. Musen, A. Das, and C. I. Nyulas, "The SWRLAPI: A development environment for working with SWRL rules," in *Proc. OWLED*, 2008, pp. 1–4.

[19] "SWRLAPI." 2021. Accessed: Jan. 25, 2022. [Online]. Available: https://github.com/protegeproject/swrlapi

[20] D. Wilkins, G. Denker, M.-O. Stehr, D. Elenius, R. Senanayake, and C. Talcott, "Policy-based cognitive radios," *IEEE Wireless Commun.*, vol. 14, no. 4, pp. 41–46, Aug. 2007.

[21] J. Redi and R. Ramanathan, "The DARPA WNAN network architecture," in *Proc. Mil. Commun. Conf.*, 2011, pp. 2258–2263.

[22] M. Sherman, A. Comba, D. He, and H. McDonald, "A cognitive policy management framework for DoD," in *Proc. Mil. Commun. Conf.*, 2010, pp. 1875–1880.

[23] B. Bahrak, J.-M. Park, and H. Wu, "Ontology-based spectrum access policies for policy-based cognitive radios," in *Proc. IEEE Int. Symp. Dyn. Spectr. Access Netw.*, Bellevue, WA, USA, Oct. 2012, pp. 489–500. [Online]. Available: http://ieeexplore.ieee.org/document/6478173/

[24] T. Ulversoy and J. Halvorsen, "An overview of policy-based spectrum management for EM systems," NATO STO, Brussels, Belgium, Rep. NATO STO SET-SCI-230, Apr. 2016. [Online]. Available: https://www.ffi.no/publikasjoner/arkiv/an-overview-of-policy-based-spectrum-management-for-em-systems

[25] R. Schrage and C. E. C. Bastidas, "The IEEE 1900.5.1 standard: Policy language for dynamic spectrum access systems," in *Proc. IEEE Int. Symp. Dyn. Spectr. Access Netw. (DySPAN)*, 2019, pp. 1–8.

[26] R. N. McDermott, "Russia's electronic warfare capabilities to 2025: Challenging nato in the electromagnetic spectrum," Int. Centre Defen. Security, Tallinn, Estonia, Rep., Sep. 2017. [Online]. Available: https://icds.ee/wp-content/uploads/2018/ICDS_Report_Russias_Electronic_Warfare_to_2025.pdf

[27] M. A. Stephens, "EDF statistics for goodness of fit and some comparisons," *J. Amer. Stat. Assoc.*, vol. 69, no. 347, pp. 730–737, Sep. 1974.

[28] J. Zhang, "Powerful goodness-of-fit tests based on the likelihood ratio," *J. Roy. Stat. Soc. B*, vol. 64, no. 2, pp. 281–294, 2002.

[29] D. Teguig, B. Scheers, and V. Le Nir, "Data fusion schemes for cooperative spectrum sensing in cognitive radio networks," in *Proc. Mil. Commun. Inf. Syst. Conf. (MCC)*, 2012, pp. 1–7.

[30] S. Koslowski, J. P. Elsner, S. Couturier, F. K. Jondral, C. Keip, and O. Bettinger, "Distributed localized interference avoidance for dynamic frequency hopping ad hoc networks," in *Proc. Wireless Innovat. Forum Conf. Commun. Technol. Softw. Defined Radio (SDR-WInnComm)*, Washington, DC, USA, 2013, pp. 1–5.

[31] T. R. Gruber, "A translation approach to portable ontology specifications," *Knowl. Acquisit.*, vol. 5, no. 2, pp. 199–220, 1993. [Online]. Available: https://www.sciencedirect.com/science/article/pii/S1042814383710083

[32] *OWL 2 Web Ontology Language Document Overview*, (2nd ed.), W3C, Wakefield, MA, USA, 2012. [Online]. Available: https://www.w3.org/TR/owl2-overview/

[33] C. R. Stevenson et al., "IEEE 802.22: The first cognitive radio wireless regional area network standard," *IEEE Commun. Mag.*, vol. 47, no. 1, pp. 130–138, Jan. 2009.

[34] T. Ulversøy and T. Maseng, "Dynamic spectrum access utilizing P2P radio node discovery: Applications to military communications," in *STO Information Systems Technology Panel (IST) Symposium Cognitive Radio and Future Networks*. Hague, The Netherlands: NCIA, May 2014.

[35] S. Bergström, J. Nilsson, U. Sterner, and U. Uppman, "Routing designs for tactical heterogeneous cooperative broadcast networks," in *Proc. Int. Conf. Mil. Commun. Inf. Syst. (ICMCIS)*, 2021, pp. 1–7.

[36] T. H. Clausen, C. Dearlove, P. Jacquet, and U. Herberg, "The optimized link state routing protocol version 2," ETSI, Sophia Antipolis, France, RFC 7181, Apr. 2014. [Online]. Available: https://rfc-editor.org/rfc/rfc7181.txt

Arne Lie (Member, IEEE) received the Ph.D. degree in telematics from the Norwegian University of Science and Technology in 2008. He is a Senior Researcher at SINTEF, Trondheim, Norway. His research interests cover radio and IP networks, and signal processing programming.

Jan Erik Håkegård received the Ph.D. degree from the Ecole Nationale Supérieure des Télécommunications, Toulouse, France, in 1997. He currently works as a Senior Researcher with SINTEF, Trondheim, Norway.

Tore Ulversøy received the Ph.D. degree in informatics from the University of Oslo, Norway, in 2011. He is currently a Research Manager with Norwegian Defense Research Establishment, Kjeller, Norway.

Vincent Le Nir received the Ph.D. degree in electronics from the National Institute of Applied Sciences, France, in 2004. He is a Senior Researcher with Royal Military Academy, Brussels, Belgium.

Ulf Sterner received the M.Sc. degree in applied physics and electrical engineering from Linköping University in 1998. He is currently a Senior Scientist with Swedish Defense Research Agency (FOI).

Anders Hansson received the M.Sc. degree in applied physics and electrical engineering from Linköping University in 1989. He is currently a Senior Scientist with Swedish Defense Research Agency (FOI).

Harri Saarnisaari (Senior Member, IEEE) is currently an Adjunct Professor with the University of Oulu, Finland. In the military communications field, his research interest cover ad hoc networks, network time synchronization, and signal processing.

Juho Markkula received the M.Sc. degree in telecommunications from the University of Oulu, Finland, in 2009, where he has been working as a Research Scientist with the Center for Wireless Communications Unit since 2008.

Tuomas Paso received the M.Sc. degree in telecommunications engineering from the University of Oulu, Finland, in 2010, where he has been working as a Research Scientist and a Project Manager since 2009.

Elisabeth Löfsved received the M.Sc. degree in applied physics and electrical engineering from Linköping University, Sweden, in 1999. She is currently a Systems Architect with Saab AB in Linköping, Sweden.

Timo Bräysy received the Ph.D. degree in physics from the University of Oulu, Finland, in 2000, where he is a Project Manager with Center for Wireless Communications Research Unit.

Jarosław Krygier received the Ph.D. degree in telecommunications from the Military University of Technology, Warsaw, Poland, in 2002, where he is currently an Assistant Professor.